Intelligent method for the helicopter turboshaft engines gas temperature determining under rapid changes in its values conditions*

Anatoliy Sachenko[1,2†], Victoria Vysotska[3,†], Serhii Vladov[4,*,†], Nataliia Vladova[5,†], and Danylo Shved[3,†]

[1] *West Ukrainian National University, Lvivska Street 11 46009 Ternopil, Ukraine*
[2] *Casimir Pulaski Radom University, Malczewskiego Street 29 26-600 Radom, Poland*
[3] *Lviv Polytechnic National University, Stepan Bandera Street 12 79013 Lviv, Ukraine*
[4] *Kharkiv National University of Internal Affairs, L. Landau Avenue 27 61080 Kharkiv, Ukraine*
[5] *Ukrainian State Flight Academy, Chobanu Stepana Street 1 25005 Kropyvnytskyi, Ukraine*

Abstract

In this paper, we propose an innovative hybrid method for the helicopter turboshaft engine's gas temperature in front of the compressor turbine, determining under rapid change conditions in operating parameters. The method is based on an adaptive neural network built on the LSTM architecture and physical and mathematical modeling implemented through a heat balance and correction using a Kalman filter combination. This approach allows us to take into account the temperature changes dynamics, compensate for the sensors' inertia and minimize the interference impact, which significantly improves the estimate accuracy compared to traditional direct measurement methods. At the signal preprocessing stage, wavelet transform and singular spectrum analysis (SSA) are used to eliminate noise and restore missing data, which ensures the initial data is high quality for further modeling. The obtained normalized data are fed to the LSTM network input equipped with an adaptation mechanism that allows adjusting the model weights depending on changes in engine characteristics. The predicted temperature values are integrated with the physical modeling results using the Kalman filter algorithm, which provides an optimal combination of information from both models in order to achieve the lowest prediction error. The method's experimental verification was carried out on the TV3-117 engine data installed on the Mi-8MTV helicopter. The obtained results demonstrate high predicting accuracy: the mean absolute error (*MAE*) was 0.34 %, the root mean square error (*RMSE*) was 0.45 %, and the determination coefficient (R^2) reached 0.992. At the same time, the algorithm's computational time does not exceed 55 ms, which allows using the method in real time for the engine operation's monitoring and diagnostics. The proposed hybrid approach has proven its efficiency in the rapidly changing conditions of operating modes, providing reliable and accurate determination of the gas temperature.

Keywords

hybrid method, LSTM, Kalman filter, neural network, adaptive modeling, gas temperature, helicopter turboshaft engine, physical and mathematical modeling, signal processing, real-time monitoring

1. Introduction

Modern helicopter turboshaft engines (TE) operate under significant dynamic loads, which requires high precision control of their operating parameters. One of the critical indicators is the gas temperature in front of the compressor turbine (TG), as it directly affects the engine's efficiency and

Intelitsis'25: The 6th International Workshop on Intelligent Information Technologies & Systems of Information Security, April 04, 2025, Khmelnytskyi, Ukraine
* Corresponding author. https://orcid.org/
† These authors contributed equally.
as@wunu.edu.ua (A. Sachenko); victoria.a.vysotska@lpnu.ua (V. Vysotska); serhii.vladov@univd.edu.ua (S. Vladov); nataliia.vladova@sfa.org.ua (N. Vladova); danylo.r.shved@lpnu.ua (D. Shved)
0000-0002-0907-3682 (A. Sachenko); 0000-0001-6417-3689 (V. Vysotska); 0000-0001-8009-5254 (S. Vladov); 0009-0009-7957-7497 (N. Vladova); 0009-0005-4306-6805 (D. Shved)

reliability [1]. However, traditional methods for measuring TG have a limited number associated with the sensor's inertia, the interference, and the presence of changing operating conditions [2]. This makes it relevant to develop intelligent methods for assessing temperature, capable of quickly adapting to changing engine dynamics.

Rapid changes in the TG, typical for the helicopter TE operation transient modes, complicate accurate measurement and require high-speed data processing algorithms [3]. Existing methods based on direct measurements often do not provide the required accuracy and stability under turbulent flows and load fluctuation conditions. An intelligent method for determining the TG using neural networks and adaptive algorithm development will improve the parameter estimation accuracy in real time, reduce the errors associated with probability with noise and systematic errors, and improve the engine's operational status prediction.

2. Related works

The TG accurate measurement issue in helicopter TEs remains relevant in the aviation industry. Traditional methods are based on thermocouple sensors, which are widely used due to their simple design and high thermal stability [4]. However, their main drawbacks are inertia, high sensitivity to vibrations and interference, as well as limited accuracy with sudden temperature changes, which make it difficult to use in dynamically changing engine operating modes. Researches [5, 6] propose improved thermocouple systems with measurement correction based on mathematical heat transfer models, but their efficiency decreases under non-stationary conditions.

An alternative to traditional methods is temperature estimation algorithms using mathematical modeling and numerical error correction methods. In [7], temperature prediction models based on heat balance equations that take into account changes in engine operating mode are proposed. However, such models require precise knowledge of engine parameters and do not always provide adaptability to real operating conditions. In [8], Bayesian methods for temperature estimation taking into account measurement uncertainties are considered, but their application is limited by the need for complex a priori calibration.

In recent years, intelligent data processing methods, including neural networks and hybrid algorithms, have been actively developed. Research [9] describes an approach using recurrent neural networks (RNN) to predict gas temperature based on time series. However, this technique does not take into account the fast transient processes typical of helicopter TE. The research [10] uses a combination of neural networks with data filtering based on wavelet transforms, which allows for increased predicting accuracy. However, most existing approaches are not adapted to the sudden temperature change conditions that occur during helicopter maneuvering and changing engine operating modes.

Despite significant progress in the TG measuring and predicting field, a number of important issues remain unresolved. Most existing methods are either focused on stationary engine operating modes [5, 6] or require complex preliminary calibrations [9, 10], which limits their application in real time. Also, the issues of comprehensively accounting for systematic and random measurement errors [7, 8] arising from turbulent disturbances and vibration loads have not been sufficiently studied.

The intelligent method for the TG assessing development based on hybrid algorithms of machine learning and mathematical modeling seems to be a promising direction. Such a method will allow taking into account the dynamics of temperature changes in transient modes, adapt to changing operating conditions, and ensure high accuracy of assessment without the need for complex adjustments. In addition, the intelligent data processing into on-board engine monitoring systems integration will significantly increase the helicopter TE operational status monitoring and predicting reliability, which is especially important for the helicopter's operation in extreme conditions.

3. Proposed method

3.1. Development of an intelligent method for the gas temperature in front of the compressor turbine estimating

The proposed method combines adaptive neural network algorithms with physical and mathematical modeling to accurately determine the TG under rapid change conditions in its values. The hybrid approach allows taking into account the temperature change dynamics, compensating for the traditional sensors' inertia and interference impact, minimizing (Figure 1).

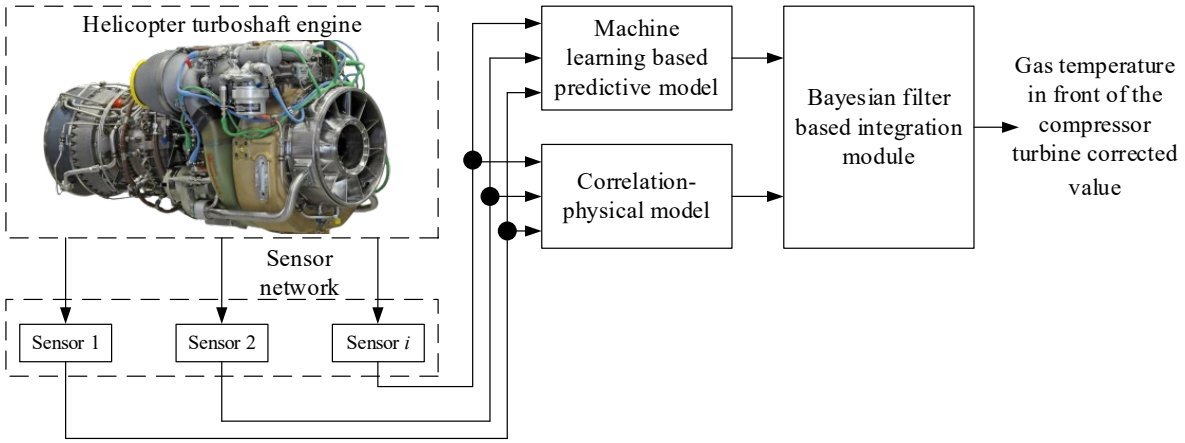

Figure 1: The proposed method structure. (author's research).

The method includes three main components: a predictive model based on machine learning, using an LSTM network with additional adaptation modules to predict temperature based on historical data and current engine operating parameters; a correlation-physical model representing an analytical description of thermal processes in helicopter TE, taking into account external factors such as operating mode, turbulence, and heat loss; and an integrating module based on a Bayesian filter, which corrects temperature estimates by combining the results of machine learning and physical modeling, ensuring high accuracy and adaptability of the method.

The proposed method architecture includes four key modules: a data preprocessing system, a neural network predicting module, a physical and mathematical model, and an integrating module (Figure 2).

The data preprocessing system cleans and normalizes signals from temperature sensors, removes noise using wavelet transform, and applies SSA (Singular Spectrum Analysis) to identify outliers and restore missing data. This ensures high quality of input data, and the noise impact reduces on subsequent processing.

The neural network predictive module is based on the LSTM (Long Short-Term Memory) architecture, trained on historical data on gas temperature, engine operating parameters (the gas-generator and free turbine rotors speed), and operating modes. It is supplemented by an adaptive learning mechanism, which allows taking into account changes in engine characteristics during operation.

equations, energy balance, and empirical coefficients and also takes into account dynamic heat losses, turbulent effects, and changes in operating modes. The integrating module, implemented on the Kalman filter basis or its nonlinear variations (for example, Unscented Kalman Filter—UKF), combines the neural network predicted data and the physical modeling results, providing a balance between accuracy and adaptability.

Weighting coefficients are adjusted in real time, which allows for changing operating conditions and increases the reliability of temperature assessment.

The physical and mathematical model calculates the TG theoretical value based on heat transfer.

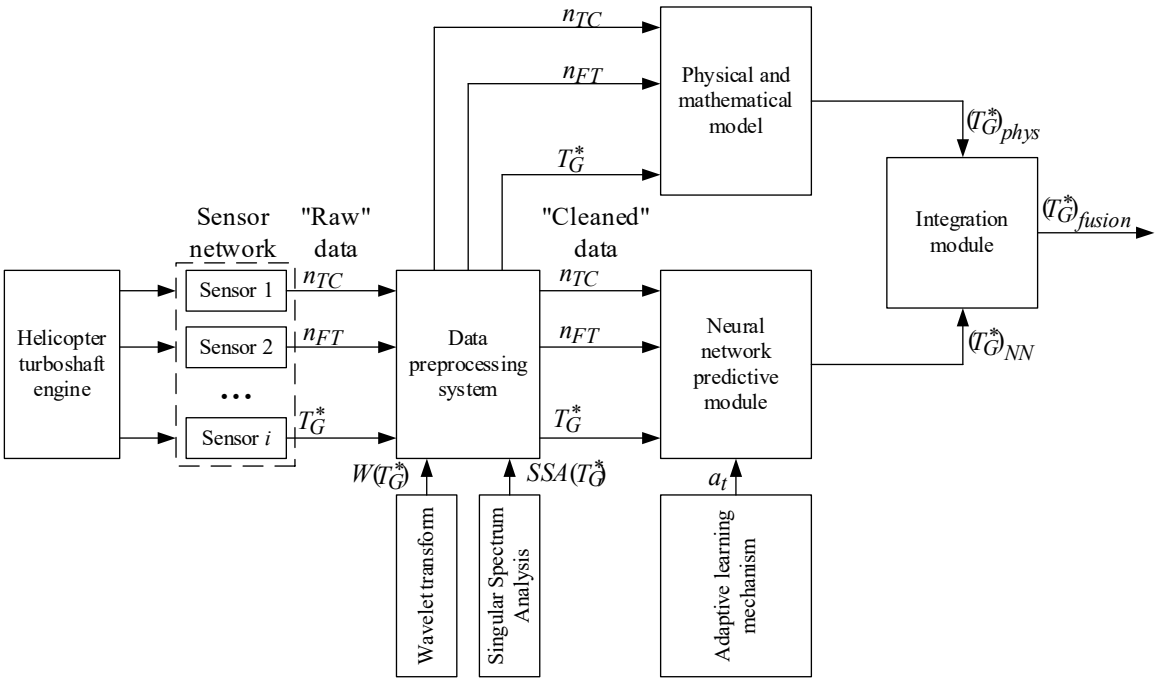

Figure 2: The proposed method architecture. (author's research).

The proposed method' algorithm is presented in Table 1.

Table 1
The results evaluating the quality of solving the missing T_G^* parameter values restoring task (author's research).

Stage number	Stage name	Stage description
1	Data collection	Receiving readings from TG sensors and auxiliary parameters (for example, the gas generator and free turbine rotor speed) [11].
2	Preliminary processing	Cleaning data from noise and outliers using wavelet filtering and SSA.
3	Predicting by neural network model	Using an LSTM network to predict the temperature for the next time step based on historical data and current parameters.
4	Calculation of physical model	The TG expected value is calculated taking into account heat transfer, energy balance, and dynamic factors.
5	Integration and correction	Using Bayesian correction (Kalman filter or UKF) to combine the neural network prediction and the physical model results.
6	Data update	Transferring the corrected values to the helicopter TE monitoring and diagnostics system for further analysis and control.

3.2. Development of a mathematical model

To develop a mathematical model describing the proposed method's architecture, several key components can be identified: a data preprocessing system, a neural network predictive module, a physical and mathematical model, and an integrating module.

Let the input data be a gas temperature measurements time series:

$$T_G^* = \left\{T_G^{*(1)}, T_G^{*(2)} \ldots, T_G^{*(i)}\right\}, \quad (1)$$

where T_G^* are the helicopter TE gas temperature in front of the compressor turbine values in time moment *t*.

Noise is removed using the wavelet transform as:

$$(T_G^*)' = W(T_G^*), \quad (2)$$

where $W(\bullet)$ is the wavelet filtering operator.

To extract the principal components, the SSA method is used in the form:

$$(T_G^*)'' = SSA((T_G^*)'), \quad (3)$$

where $SSA(\bullet)$ is the decomposition operator into a singular spectrum and restoration of the useful signal.

Signal preprocessing includes denoising and data normalization. Signal filtering is used to denoise the signal, and *z*-normalization is used for the denoised signal [12]:

$$z(T_G^*)''_{(i)} = \frac{(T_G^*)''_{(i)} - \frac{1}{N} \cdot \sum_{i=1}^{N} (T_G^*)''_{(i)}}{\sqrt{\frac{1}{N} \cdot \sum_{i=1}^{N} \left((T_G^*)''_{(i)} - \frac{1}{N} \cdot \sum_{i=1}^{N} (T_G^*)''_{(i)}\right)^2}}, \quad (4)$$

where *N* is the training dataset size. The *z*-normalization use allows us to the variables T_G^* each value transform so that they are expressed in standard deviation units from the mean. This allows us to bring the T_G^* data to a form with a mean value of 0 and a standard deviation of 1, which is important for improving the machine learning algorithms convergence and for the data correct comparison with different scales.

The LSTM based network prediction can be represented as follows:

$$h_t = LSTM\left(h_{t-1}, (T_G^*)''_{(i)}, \alpha_t\right), \quad (5)$$

where $(T_G^*)''_{(i)}$ is the input vector containing gas temperature in front of the compressor turbine normalized data, h_t is the hidden state at time *t*, α_t is an adaptation coefficient that takes into account changes in engine characteristics. The adaptation coefficient α_t describes the added adaptive learning mechanism that changes the weights in the neural network depending on changes in engine characteristics.

To calculate the T_G^* theoretical value, a thermodynamic model is used based on the energy balance and compression and combustion processes equations [13].

The power transferred to the gas flow is determined by the equation:

$$Q_f = m_f \cdot H_u \cdot \eta_G, \quad (6)$$

where Q_f is the thermal power released during fuel combustion, W; m_f is the fuel mass flow rate, kg/s; H_u is the fuel net calorific value, J/kg; η_G is the combustion process efficiency (usually 0.96…0.99).

The gas temperature in front of the compressor turbine is determined from the heat balance equation:

$$m_{air} \cdot c_p \cdot T_{air} + m_f \cdot c_{pt} \cdot T_f + Q_f = \left(m_{air} + m_f\right) \cdot c_p \cdot T_G^*, \quad (7)$$

wherefrom

$$T_G^* = \frac{m_{air} \cdot c_p \cdot T_{air} + m_f \cdot c_{pt} \cdot T_f + Q_f}{\left(m_{air} + m_f\right) \cdot c_p}, \tag{8}$$

where m_{air} is the air mass flow rate, kg/s; T_{air} is the air temperature in front of the combustion chamber, K; c_p is the gas specific heat capacity at constant pressure, J/(kg K); c_{pt} is the fuel specific heat capacity, J/(kg K); T_f is the fuel temperature, K.

If we neglect the fuel heat capacity ($c_{pt} \approx c_p$), then (8) is simplified to:

$$T_G^* = T_{air} + \frac{m_f \cdot H_u \cdot \eta_G}{\left(m_{air} + m_f\right) \cdot c_p}. \tag{9}$$

This physical model shows that the gas temperature in front of the compressor turbine is determined by the temperature of the incoming air, the fuel combustion heat, and the combustion chamber efficiency.

To adjust the neural network and the physical model predictions, the Unscented Kalman Filter (UKF) [14] is used. It is assumed that x_t is the system's current state, z_t is the observed value, A is the state matrix, H is the observation matrix, P_t is the state error covariance matrix, Q is the process covariance matrix, R is the measurement covariance matrix, and K_t is the Kalman matrix (update weighting factor).

The UKF algorithm consists of two stages: the predicting stage and the correction stage. At the predicting stage, sigma points are formed, the predicted sigma points are determined, and the state and covariance predictions are made as:

$$\begin{gathered}
\chi_{t-1}^i = x_{t-1} + W_i \cdot \sqrt{(n+\lambda) \cdot P_{t-1}}, \qquad i = 0, \ldots, 2n, \\
\chi_t^i = f\left(\chi_{t-1}^i\right) + \omega_t^i, \omega_t^i \sim N(0, Q), \\
\hat{x}_t = \sum_{i=0}^{2n} W_i \cdot \chi_t^i, \\
P_t = \sum_{i=0}^{2n} W_i \cdot \left(\chi_t^i - \hat{x}_t\right) \cdot \left(\chi_t^i - \hat{x}_t\right)^T + Q,
\end{gathered} \tag{10}$$

where W_i is the sigma points weights, λ is the scaling parameter, n is the state dimension.

At the correction stage, the sigma points projection onto the measurement space, measurement prediction, measurement covariance, cross-covariance, Kalman matrix determination, and state and covariance matrix updating are performed as:

$$\begin{gathered}
\zeta_t^i = h\left(\chi_t^i\right) + v_t^i, v_t^i \sim N(0, R), \\
\hat{z}_t = \sum_{i=0}^{2n} W_i \cdot \zeta_t^i, \\
S_t = \sum_{i=0}^{2n} W_i \cdot \left(\zeta_t^i - \hat{z}_t\right) \cdot \left(\zeta_t^i - \hat{z}_t\right)^T + R, \\
P_{xz} = \sum_{i=0}^{2n} W_i \cdot \left(\zeta_t^i - \hat{z}_t\right) \cdot \left(\zeta_t^i - \hat{z}_t\right)^T, \\
K_t = P_{xz} \cdot S_t^{-1}, \\
x_t = \hat{x}_t + K_t \cdot (z_t - \hat{z}_t), \\
P_t = P_t - K_t \cdot S_t \cdot K_t^T.
\end{gathered} \tag{11}$$

The neural network predicts and the physical model results combination using the Unscented Kalman Filter (UKF) is carried out as follows:

$$(T_G^*)_{fusion} = K_t \cdot (T_G^*)_{NN} + (I - K_t) \cdot (T_G^*)_{phys}, \quad (12)$$

where $(T_G^*)_{fusion}$ is the gas temperature in front of the compressor turbine combined predicted value, $(T_G^*)_{NN}$ is the predicted value obtained by the LSTM network (equation 5), $(T_G^*)_{phys}$ is the value calculated using the thermodynamic model (equation 9), K_t is the Kalman matrix, which determines the neural network prediction and the physical model weight adaptation (11).

Thus, the final predict is formed as a data adaptive combination from the physical model and neural network prediction, where the weighting coefficient K_t takes into account the trust in each source of information.

3.3. Development of a neural network predictive module

The predictive module is designed to predict the gas temperature in front of the compressor turbine T_G^* based on historical data on temperature, engine operating parameters, and operating modes. The module is based on an LSTM network that adapts to changes in engine characteristics during operation. The predictive module model architecture includes the following main components: input layer, LSTM layer, fully connected layer, output layer (Figure 3).

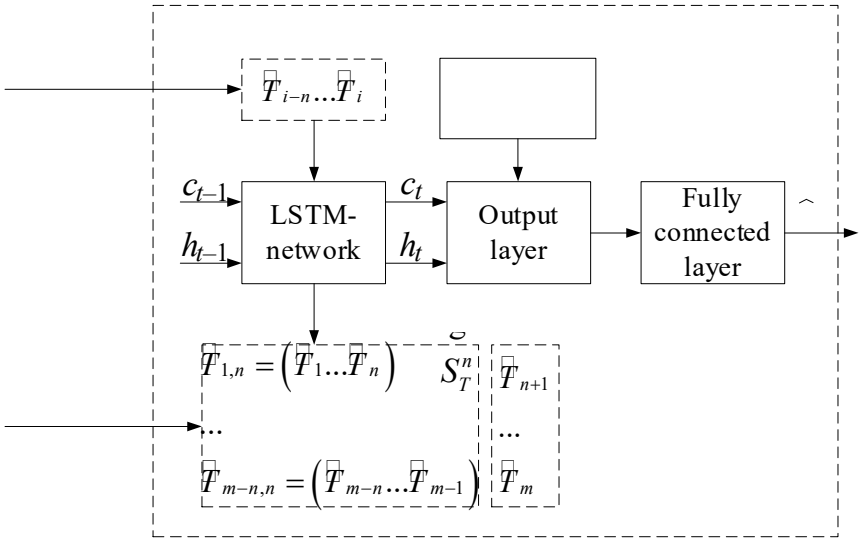

Figure 3: The predictive module architecture. (author's research).

The input layer receives the parameters of the time series recorded by the standard sensors on board the helicopter: gas temperature in front of the compressor turbine T_G^*, gas-generator rotor speed n_{TC}, free turbine rotor speed n_{FT}, and the adaptation coefficient α_t value. The LSTM layer with the hidden state dimension h_t includes forgetting and remembering mechanisms for analyzing long time dependencies. The fully connected layer transforms the LSTM output into the predicted temperature $\hat{T}_G^*$. The output layer produces the gas temperature in front of the compressor turbine predicted value.

Each LSTM node consists of three main gates: forget, input, and output. For a time moment t, the LSTM cell (Figure 4) state is updated by defining the input data vector x_t, defining the forget gate (determines how much information from the previous state should be forgotten) f_t, the input gate (determines how much new information should be added) i_t, the cell state update candidate $\tilde{c}_t$, the cell state update c_t, the output gate o_t, and the hidden state update h_t [15, 16]:

$$x_t = \left\{T_G^{*(t-1)}, n_{TC}^{(t-1)}, n_{FT}^{(t-1)}, \alpha_t\right\}, \quad (13)$$

$$f_t = \sigma(W_f \cdot x_t + U_f \cdot h_{t-1} + b_f),$$
$$i_t = \sigma(W_i \cdot x_t + U_i \cdot h_{t-1} + b_i),$$
$$\tilde{c}_t = \tanh(W_c \cdot x_t + U_c \cdot h_{t-1} + b_c),$$
$$c_t = f_t \cdot c_{t-1} + i_t \cdot \tilde{c}_t,$$
$$o_t = \sigma(W_o \cdot x_t + U_o \cdot h_{t-1} + b_o),$$
$$h_t = o_t \cdot \tanh(c_t),$$

where W, U, b are the model' trainable parameters, $\sigma(\bullet)$ is the sigmoid activation function.

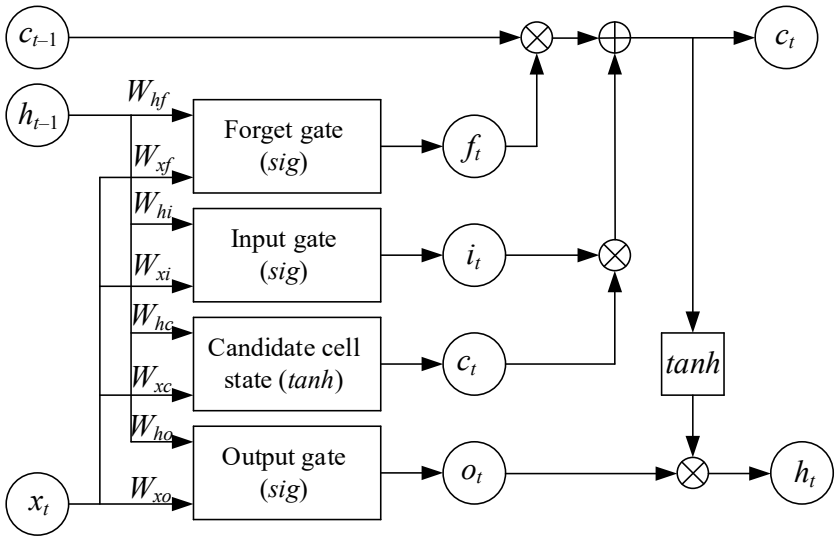

Figure 4: The LSTM network diagram. [15, 16].

The predictive module' output layer generates the gas temperature in front of the compressor turbine predicted value as:

$$\hat{T}_G^* = W_h \cdot h_t + b_h. \tag{14}$$

Next, the T_G^* predict is transferred to the integrating module, where it is combined with the physical model result according to (12).

The LSTM network is supplemented with an adaptation mechanism that allows adjusting weights when engine characteristics change. The adaptation coefficient α_t adjusts the input parameters influence that depends on the engine age and operating conditions and is used when updating the neural network weights, affecting the training speed. The adaptation coefficient α_t is determined by the measured deviation parameters δT_G^*, δn_{TC}, δn_{FT} as:

$$\alpha_t = (\delta T_G^*, \delta n_{TC}, \delta n_{FT}). \tag{15}$$

Thus, the neural network predictive module uses transfer training, in which, when new data is available, the model is partially retrained using weight adjustment methods.

Thus, the proposed method's scientific novelty lies in the hybrid intelligent approach development to estimating the gas temperature in front of the compressor turbine under rapidly changing value conditions. Unlike traditional methods based on direct measurements using thermocouples, the proposed method combines adaptive neural network algorithms with physical and mathematical modeling, which allows taking into account the temperature change dynamics, compensating for the sensor's inertia, and minimizing the interference impact.

The method' key innovations include:

1. A hybrid approach combining LSTM recurrent neural network predicting and thermodynamic modeling with UKF Kalman filter correction;

2. An intelligent adaptation mechanism that takes into account changes in engine performance during operation, which improves the assessment accuracy without the need for complex calibration;
3. Efficient data processing, including wavelet filtering and singular spectrum analysis (SSA) to eliminate noise and restore missing values;
4. Real-time implementation, providing high processing speed and the ability to integrate into on-board helicopter TE monitoring and diagnostic systems.

This method use helps to increase the gas temperature reliability assessment in front of the compressor turbine, reduce the measurement errors probability and improve predictive diagnostics of the helicopter TE operational status.

4. Results

4.1. The input data analysis and preprocessing

To conduct a computational experiment demonstrating the developed method's operability, this research object was the TV3-117 engine [17], which is part of the Mi-8MTV helicopter and its modifications to the power plant. Based on the Mi-8MTV helicopter flight test results, data on the TV3-117 engine parameters were obtained and recorded on board the helicopter by standard sensors of the onboard monitoring system: the gas temperature in front of the compressor turbine T_G^* (a sensor consisting of 14 dual thermocouples T-101 was used), the gas-generator rotor speed n_{TC} (a D-2M sensor was used), and the free turbine rotor speed n_{FT} (a D-1M sensor was used) [18]. The data on board the Mi-8MTV helicopter were recorded during a real flight for 320 seconds with a sampling frequency of 0.25 seconds. To form time series from flight data of the onboard engine parameter monitoring system TV3-117, the measurements' sequential processing obtained from standard sensors T-101, D-2M, and D-1M is performed.

The initial data T_G^*, n_{TC}, n_{FT} (1) underwent preliminary processing, including noise reduction and outliers' elimination (2), (3), after which time series are formed—ordered sequences of parameter values over time. To reduce time series with parameters' different scales to a single scale, z-normalization is applied (4). After normalization, the parameters T_G^*, n_{TC}, n_{FT} time series have the form shown in Figure 5.

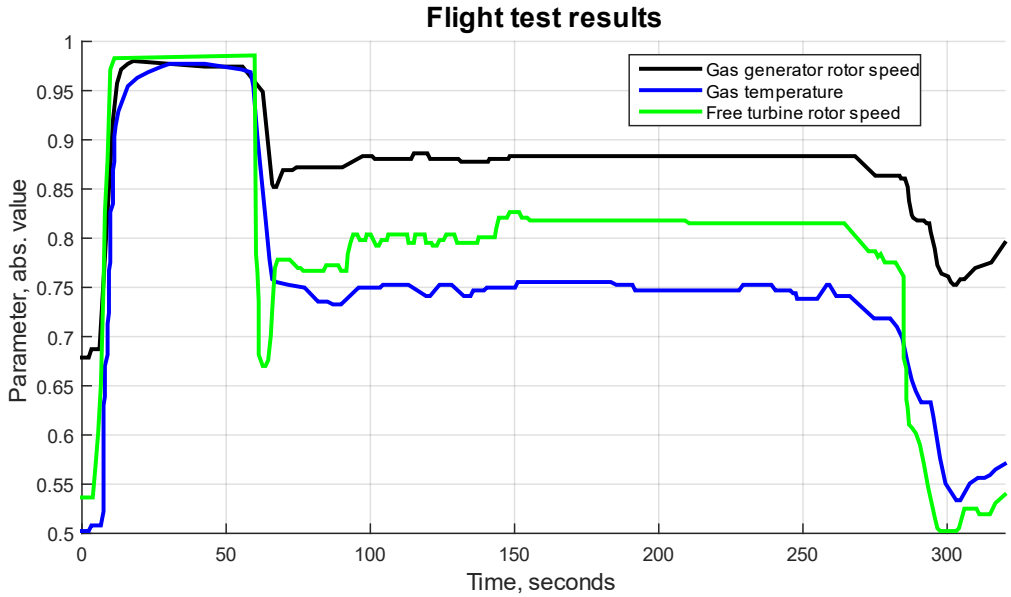

Figure 5: The TV3-117 engine normalized parameters time series diagrams: "black curve" is the gas-generator rotor speed n_{TC}, "blue curve" is the gas temperature in front of the compressor turbine T_G^*, "green curve" is the free turbine rotor speed n_{FT} (author's research).

Based on the presented diagrams, a parameters' T_G^*, n_{TC}, n_{FT} training dataset was formed, which fragment is presented in Table 2.

Table 2
The parameters' T_G^*, n_{TC}, n_{FT} normalized values training dataset fragment (author's research)

Number	The gas temperature in front of the compressor turbine T_G^*	The gas-generator rotor speed n_{TC}	The free turbine rotor speed n_{FT}
1	0.995	0.989	0.988
…	…	…	…
166	0.983	0.976	0.974
…	…	…	…
251	0.986	0.978	0.976
…	…	…	…
375	0.973	0.964	0.96
…	…	…	…
492	0.986	0.978	0.977
…	…	…	…
630	0.980	0.975	0.974
…	…	…	…
789	0.987	0.981	0.979
…	…	…	…
985	0.991	0.989	0.986
…	…	…	…
1280	0.993	0.990	0.987

To assess the parameters T_G^*, n_{TC}, n_{FT} training dataset homogeneity, based on [19], the Fisher-Pearson criterion χ^2 general statistics was used. To draw a conclusion, the calculated χ^2 indicator is compared with the threshold value corresponding to the specified significance level α and the number of degrees of freedom (in this case, 2). If $\chi^2 > \chi^2_{critical}(\alpha, 2)$, the normal distribution assumption is rejected. In this study, the significance level $\alpha = 0.01$ was set, which is due to strict requirements for helicopter flight safety [20]. The false assumption of erroneous acceptance probability minimizing (for example, missing a deviation from the norm) plays a key role in preventing emergency situations. This significance level increases the reliability of the decisions made and reduces the likelihood of engine failures in flight. Table 3 presents the parameters T_G^*, n_{TC}, n_{FT} training dataset homogeneity estimating results according to the Fisher-Pearson criterion.

Table 3
Results of the parameters' T_G^*, n_{TC}, n_{FT} training dataset training dataset homogeneity assessing according to the Fisher-Pearson criterion (author's research)

Parameter	The χ^2 calculated value	The $\chi^2(\alpha, 2)$ critical value	Decision on the training dataset homogeneity
T_G^*	9.134	9.2	The dataset is homogeneity.
n_{TC}	9.147		
n_{FT}	9.183		

The training dataset homogeneity, according to [21], is checked using the Fisher-Snedecor criterion F_{ij}. To assess the parameters T_G^*, n_{TC}, n_{FT} consistency, their variances are compared pairwise. The F_{ij} calculated values are compared with the threshold value $F_{critical}$, set for a given significance level $\alpha = 0.01$ and degrees of freedom $\nu_1 = N_1 - 1$ and $\nu_2 = N_2 - 1$ (where $N_1 = N_2 = N = 1280$ are the

datasets sizes). If $F_{ij} > F_{critical}$, the datasets are considered heterogeneous. Table 4 presents the parameters T_G^*, n_{TC}, n_{FT} training dataset homogeneity, confirming results according to the Fisher-Snedecor criterion.

Table 4

Results of the parameters' T_G^*, n_{TC}, n_{FT} training dataset training dataset homogeneity assessing according to the Fisher-Snedecor criterion (author's research)

Parameter	The F_{ij} calculated value	The $F_{critical}(\alpha = 0.01, 1279)$ critical value	Decision on the training dataset homogeneity
T_G^*	1.129	1.139	The dataset is homogeneity
n_{TC}	1.132		
n_{FT}	1.133		

To check the training dataset's representativeness, the cluster analysis method (k-means [22]) was used. Within this approach framework, the training and test datasets were formed by random partitioning in a 2:1 ratio (67 and 33 %, respectively, which corresponds to 858 and 422 elements). The training dataset (Table 2) clustering results showed the 8 groups (classes I...VIII) presence, which indicates the eight clusters identification and confirms the training and test datasets structure similarity (Figure 6).

Based on these data, the optimal dataset sizes for signals from the TV3-117 engine T-101, D-2M, and D-1M sensors were determined: training dataset is 1280 elements (100 %), control dataset is 858 elements (67 % of the training dataset), test dataset is 422 elements (33 % of the training dataset).

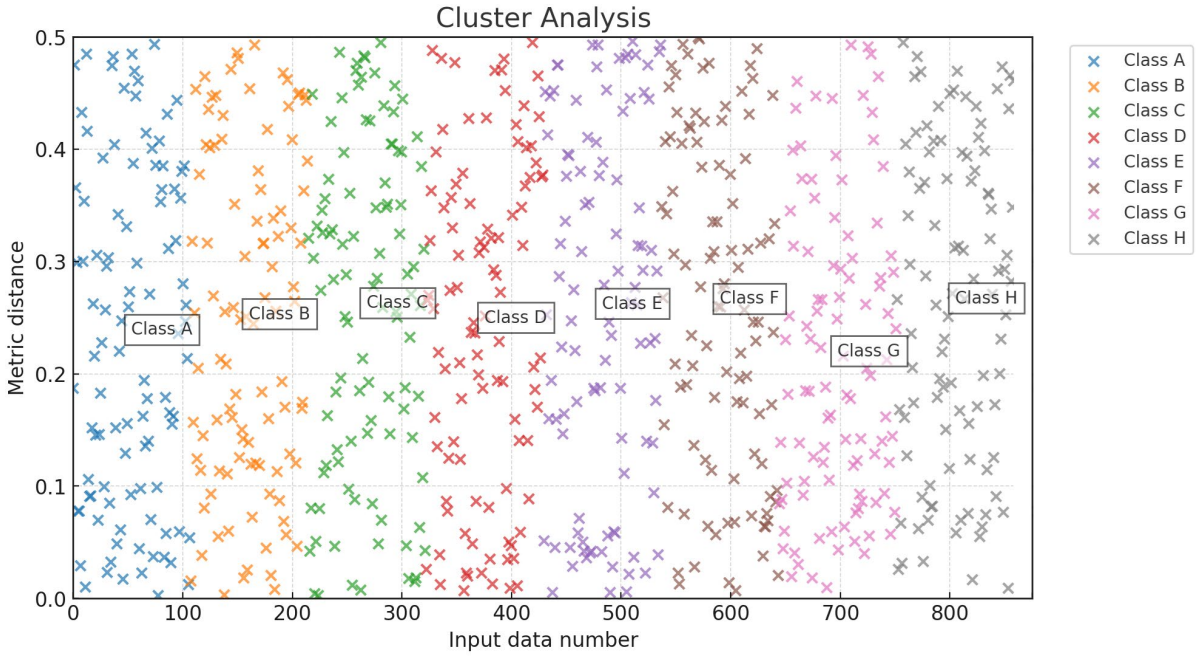

a

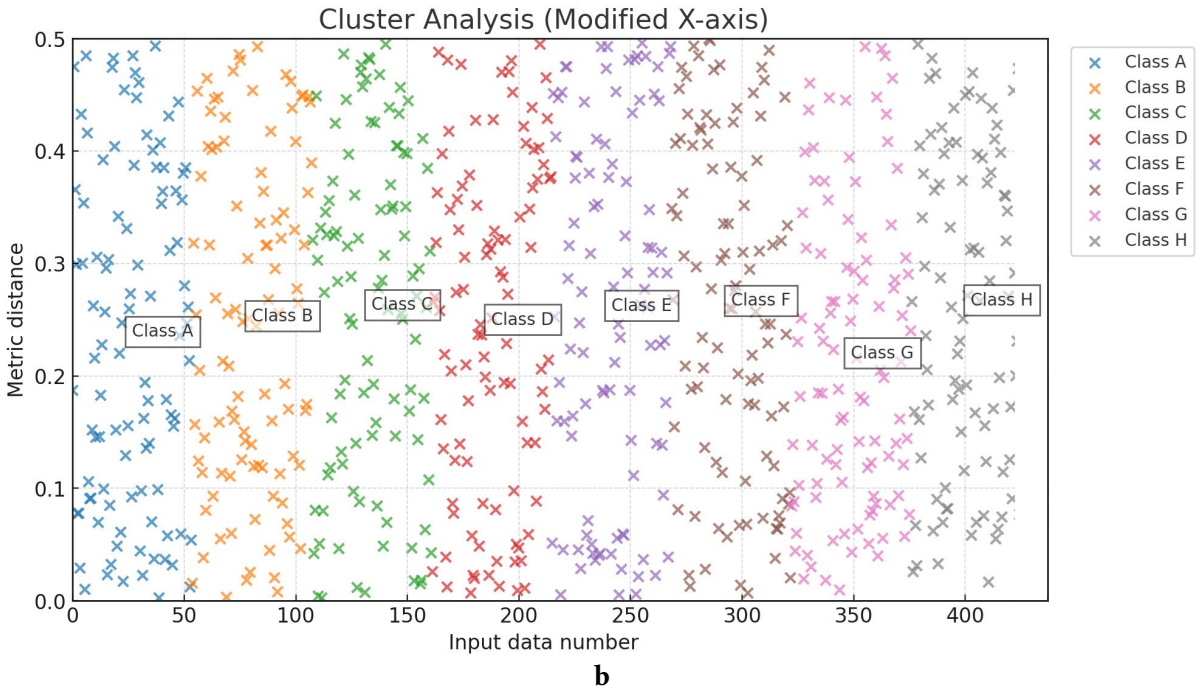

b

Figure 6: Cluster analysis results: **a** is the training dataset; **b** is the test dataset. (author's research).

4.2. The method' performance testing results

To adapt the developed method to transient engine operation modes, Figure 7 shows a diagram of transient processes for the gas temperature in front of the compressor turbine T_G^* parameter. In Figure 7, the black solid line shows the T_G^* data from the T-101 sensor, containing jumps and noise, the red dotted line shows the predicted T_G^* data using a neural network model (LSTM) curve, demonstrating possible delays or errors, the blue dashed-dotted line shows the corrected temperature T_G^* curve, demonstrating the final value after the Kalman filter, showing the adaptation of the method to rapid changes.

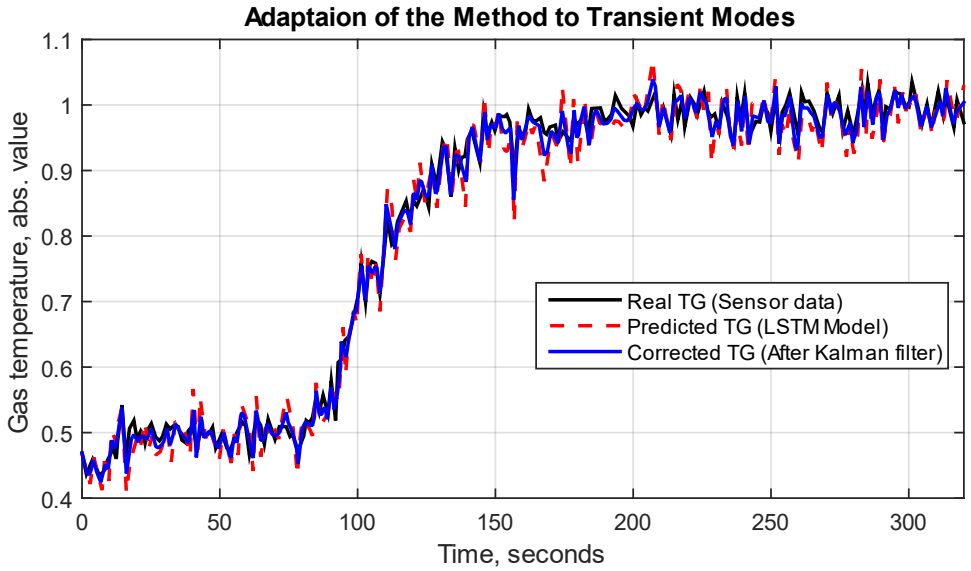

Figure 7: The method' adaptation to transient modes diagram. (author's research).

This diagram clearly shows how the LSTM neural network model and the Kalman filter's sequential application improve the gas temperature data in front of the compressor turbine quality. The original (black) curve contains noise and jumps, which complicate the analysis. The predicted

(red) line already smooths out some of the noise but may have delays or errors. The final (blue) curve after the Kalman filter eliminates jumps and "fits" the result to real measurements while maintaining a smooth shape.

Figure 8 shows the prediction root mean square error (*RMSE*) dependence on the adaptive coefficient α_t. Figure 8 compares two models: without adaptation (red dotted line) and with adaptation (blue solid line). It is evident that with the α_t growth, the adaptive model's RMSE decreases monotonically, indicating an improvement in the prediction accuracy due to the adaptation mechanism use. In contrast, the model without adaptation demonstrates higher and fluctuating RMSE values, indicating a lower ability to adapt to changing conditions.

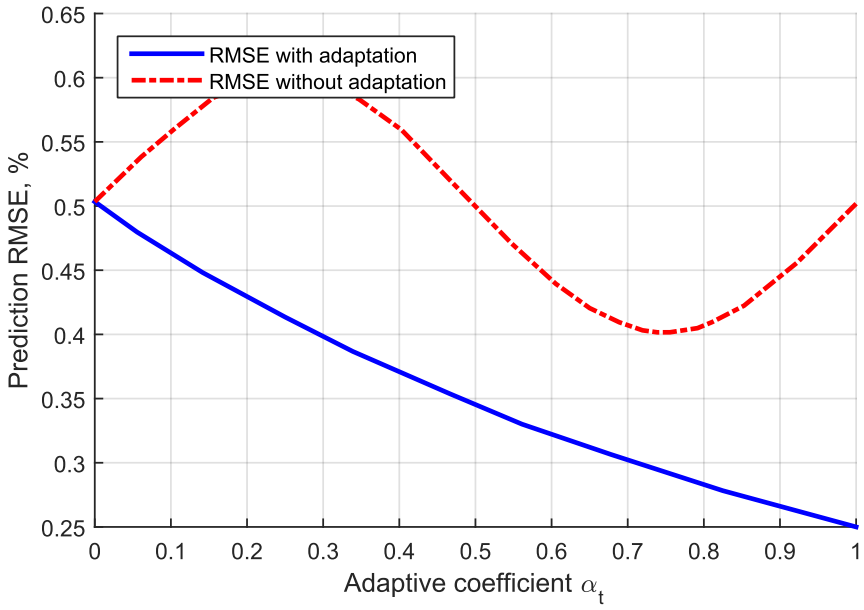

Figure 8: Diagram of the adaptive coefficient influence on the prediction' accuracy. (author's research).

Figure 9 shows the change in the temperature derivative $\frac{\partial T_G^*}{\partial t}$ over time in transient modes, where three curves are compared: the actual rate of temperature change predicted by the neural network model and the corrected rate after applying filtering. This approach allows us to visually assess how well the model predictions correspond to the real data, as well as to show the effectiveness of filtering in eliminating noise and the measurements accuracy increasing when analyzing dynamic temperature transitions.

The diagram shows that the actual rate of temperature change (blue line) has a pronounced maximum in the middle of the range (around t = 320), forming a smooth bell-shaped curve. The rate predicted by the neural network (red line) follows the actual curve's general shape but contains noticeable noise and deviations, especially near the peak. After applying filtering (green dotted line), the noise is significantly reduced, and the curve becomes smoother, while the main dynamics of the actual rate of temperature change are preserved.

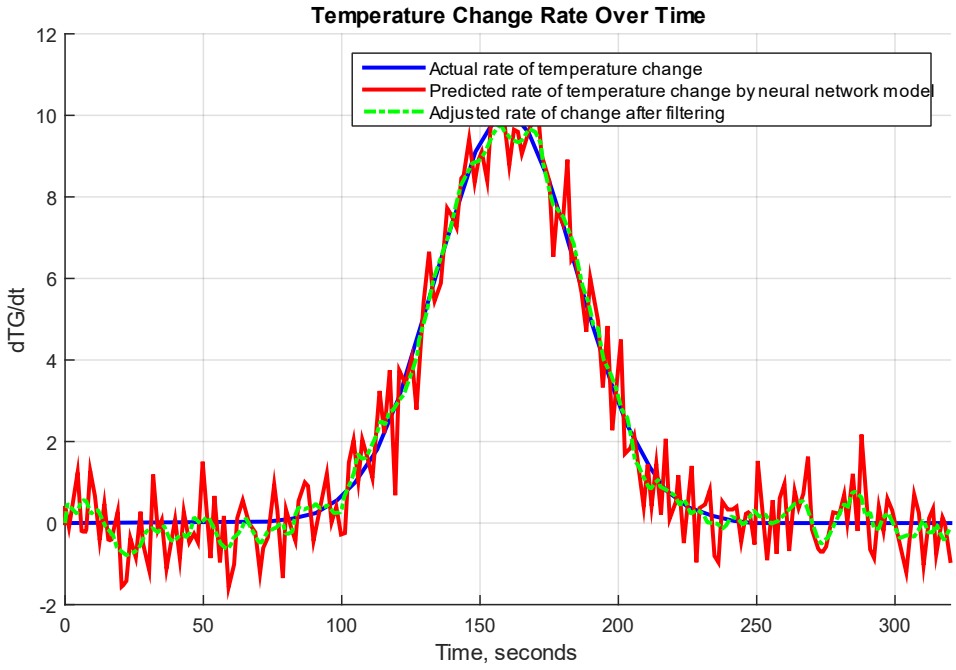

Figure 9: Diagram of the change in the temperature derivative over time. (author's research).

4.3. The results obtained effectiveness evaluation

To evaluate the different algorithms' computation time, the computation time was measured for three algorithms used to estimate the gas temperature in front of the compressor turbine. The experiment was conducted on typical hardware using a semi-naturalistic simulation stand [23], under equal testing conditions, using both real and synthetically generated data simulating the engine operating dynamics. Each algorithm was run multiple times, and the average computation time was determined to reduce the random errors influence. According to the obtained results, the LSTM model showed the shortest running time—about 22 ms—which is due to the time series efficient processing and optimized network architecture. The physical and mathematical model implementing calculations based on heat balance and energy exchange equations required about 37 ms, as it included more complex mathematical operations. The combined method integrating the LSTM model with the physical-mathematical model through the use of the Kalman filter for prediction correction had the longest computation time—about 55 ms—which is explained by processing' additional stages and results' adaptation. The obtained results (Table 5) demonstrate that even the most resource-intensive approach remains within the acceptable time for real-time operation, which is critical for the method implementation in helicopter TE onboard monitoring and diagnostic systems.

Table 5

Results of the parameters' T_G^*, n_{TC}, n_{FT} training dataset training dataset homogeneity assessing according to the Fisher-Pearson criterion (author's research)

Algorithm Type	Computation Time (ms)
LSTM Model	22
Physical-Mathematical Model	37
Combined Method	55

At the next stage, data on gas temperature in front of the compressor turbine T_G^* prediction errors were collected for each of the three algorithms: the LSTM model, the physical-mathematical model, and the combined method. For each method, the difference between the predicted values $(T_G^*)_{pred}$ and the real measurements $(T_G^*)_{real}$ was calculated for a test observations number. The obtained errors were distributed over a values range, and an error histogram was obtained for each algorithm (Figure 10), displaying the observations number depending on the error value. Thus, the error histogram can be used to estimate which error distribution is typical for each approach: for example, a narrow distribution with a smaller variance indicates an algorithm's higher accuracy, while a wide distribution indicates a larger spread of errors.

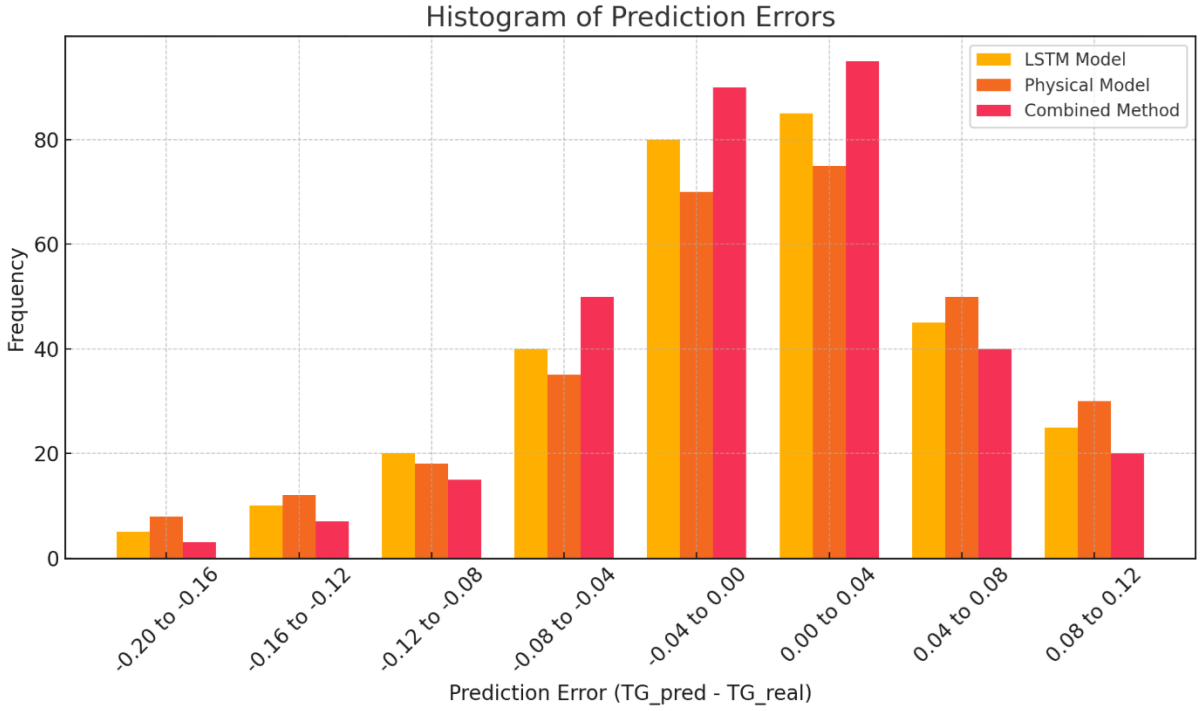

Figure 10: The prediction errors histogram. (author's research).

As can be seen from Figure 10, the errors histogram obtained using the LSTM model shows a relatively narrow distribution with a small spread, indicating high prediction accuracy in most cases. The physical-mathematical model's errors histogram is more diffuse, reflecting the complex physical calculations influence, where the values spread is somewhat larger. The combined method histogram shows the distribution obtained by integrating the two approaches using the Kalman filter result, which allows for a decrease in the overall prediction error and a decrease in the spread.

At the final stage, the predictive model's efficiency and quality are assessed according to traditional metrics. In this case, efficiency can be understood as, for example, the mean absolute error (*MAE*) or the root mean square error (*RMSE*), and quality is the determination coefficient (R^2) [24]. The mean absolute error shows the average absolute deviation of predictions from real values, while the root mean square error amplifies the large errors impact. The determination coefficient shows how well the model explains the data variability. These metrics are defined as:

$$MAE = \frac{1}{N} \cdot \sum_{i=1}^{N} \left| (T_G^*)_{pred}^{(i)} - (T_G^*)_{real}^{(i)} \right|, RMSE = \sqrt{\frac{1}{N} \cdot \sum_{i=1}^{N} \left((T_G^*)_{pred}^{(i)} - (T_G^*)_{real}^{(i)} \right)^2}, \quad (14)$$

$$R^2 = 1 - \frac{\frac{1}{N} \cdot \sum_{i=1}^{N} \left((T_G^*)_{pred}^{(i)} - (T_G^*)_{real}^{(i)} \right)^2}{\frac{1}{N} \cdot \sum_{i=1}^{N} \left((T_G^*)_{real}^{(i)} - \left(\overline{T}_G^* \right)_{real} \right)^2},$$

where $(T_G^*)_{pred}^{(i)}$ is the gas temperature predicted value, $(T_G^*)_{real}^{(i)}$ is the actual measured value, $\left(\overline{T}_G^* \right)_{real}$ is the actual measurements average value.

Based on the calculations carried out on the grouped error intervals basis, the *MAE*, *RMSE* and R^2 metrics values were obtained (Table 6).

Table 6
Results of calculating *MAE*, *RMSE* and R^2 metrics. (author's research).

Metric	LSTM Model	Physical Model	Combined Method
MAE, %	0.49	0.53	0.34
RMSE, %	0.62	0.67	0.45
R^2	0.987	0.976	0.992

From these results, it is evident that the combined method gives the lowest *MAE*, *RMSE*, and R^2, which is consistent with the finding of higher accuracy and smaller error spread compared to the other two models.

5. Discussions

An intelligent method for estimating the helicopter TE gas temperature in front of the compressor turbine has been developed (Figures 1 and 2), which combines adaptive neural networks and physical and mathematical modeling to obtain accurate results under dynamic changes. The method includes a predictive model based on LSTM with adaptive modules, a correlation-physical model for describing thermal processes taking into account energy exchange, turbulence and dynamic losses, as well as an integrating module based on a Bayesian filter (for example, a Kalman filter or its nonlinear variants) for adjusting predicted values. Preliminary data processing using wavelet transform and SSA provides signal cleaning and normalization, minimizing the noise influence, which in turn increases the gas temperature estimate accuracy and adaptability, making the method effective for the helicopter TE operation's monitoring and diagnosing.

Within the developed method (Figures 1 and 2) framework, a mathematical model for the helicopter TE gas temperature in front of the compressor turbine was developed, which is based on the temperature measurements time series processing (1), after which noise is removed using a wavelet transform (2), and the main components are identified using singular spectrum analysis (3). Further data normalization (4) improves the algorithm's convergence, and predicting is implemented through an LSTM network taking into account the adaptive change in engine characteristics (5). In parallel, a physical model based on the heat balance and combustion equations (6)–(9) is used, and the final prediction is formed by adaptively combining the results of both models using a Kalman filter, where the adjustment is made at the prediction and correction stages (10)–(12). The prediction is implemented using an LSTM network (Figures 3 and 4), the hidden state of which is updated according to calculations (13) with the final prediction given by (14), and the result is adjusted using a physical model based on the heat balance and combustion efficiency equations (6)–(9), where the combination of predictions is carried out using the Kalman filter (10)–(12). Additionally, the coefficient adaptation α_t (15) allows dynamic adjustment of the changing engine characteristics influence on the model.

A computational experiment was conducted to evaluate the developed method's efficiency for predicting the gas temperature in front of the compressor turbine, based on the LSTM model and the physical-mathematical model using the Kalman filter (10)–(12) combination. The experiment was

carried out on data obtained during the Mi-8MTV helicopter' TV3-117 engine real flight tests (Figure 5), where pre-processing included noise removal, selection of the time series main components and normalization (Table 2).

During the experiment, it was found that the correction stage with the Kalman filter use allows for significant smoothing of jumps and delays in predictions, ensuring the method's adaptation to transient engine operating modes (Figure 7). The *RMSE* dependence analysis on the adaptive coefficient α_t (Figure 8) showed a monotonic decrease in error, which confirms the implemented adaptive mechanism effectiveness.

The predicted quality by the *MAE*, *RMSE* and R^2 metrics final assessment (Table 6) demonstrated that the combined method provides the best results: *MAE* was 0.34 %, *RMSE* was 0.45 %, and the determination coefficient R^2 reached 0.992. At the same time, the computation time does not exceed 55 ms, which allows using the developed method in real time for monitoring and diagnosing the operation of aircraft engines.

At the same time, the obtained results have a number of limitations:

1. The experimental results were obtained using data from one specific engine (TV3-117), which limits the method applicability to other models or types of helicopter TE.
2. The final estimate's accuracy depends significantly on the preliminary signal processing (wave transform, SSA, normalization) quality, and even minor errors at this stage can negatively affect the results.
3. The combined method, although demonstrating the lowest error rates, has a higher computational complexity (about 55 ms), which can become a limiting factor in systems with very strict response time requirements.
4. The neural network adaptation mechanism operation depends on the correct determination of the adaptation coefficient α_t, and its incorrect configuration can lead to a decrease in the prediction's accuracy with abrupt changes in engine characteristics.

To eliminate these limitations, the following prospects for further research are proposed:

1. Conducting additional tests on various types of engines to verify the method generalizability.
2. Improving the signal pre-processing stage (wave transform, SSA, normalization) to increase the results stability.
3. Optimizing the computational algorithms of the combined method, for example, [25], to reduce the response time in systems with strict time constraints.
4. Developing and testing an improved adaptation mechanism for correctly determining the adaptation coefficient α_t with abrupt changes in engine characteristics.

6. Conclusions

A method has been developed that is a hybrid approach that combines an adaptive neural network based on the LSTM architecture with physical and mathematical modeling using heat balance equations and correction using the Kalman filter. This combination allows taking into account the gas temperature dynamics changes under engine operating modes' rapid transition' conditions, compensating for the sensors' inertia and the interference impact minimizing, which is a significant advantage compared to traditional direct measurement methods.

The experiments conducted on the TV3-117 engine data installed on the Mi-8MTV helicopter demonstrated high predicting accuracy. The main quality metrics (*MAE*, *RMSE*, and the determination coefficient R^2) showed that the combined method achieves *MAE* values of 0.34 %, *RMSE* is 0.45 % and R^2 is 0.992, which indicates a decrease in errors and a decrease in the errors' spread compared to individual approaches. At the same time, the algorithm's computational time, not exceeding 55 ms, confirms its possibility of using it in real time for monitoring and diagnosing engine operation.

The adaptive mechanism implemented through the coefficient αt allows the system to quickly respond to changes in engine characteristics, ensuring the neural network weights and the predicted data integration with the physical modeling results adjustment. The Kalman filter's use helps smooth out emissions and eliminate delays in predictions, which increases the final estimate's reliability. This approach significantly improves the temperature assessment quality and ensures the system's stability even with rapid mode transitions under conditions.

Thus, the developed method demonstrates high efficiency and accuracy in estimating the gas temperature in front of the compressor turbine, which is an important factor for increasing the helicopter TE reliability. The results obtained confirm the using hybrid algorithms prospects to solve real-time problems, and experimental further optimization and expansion base can contribute to its implementation in helicopter TE on-board monitoring systems.

Acknowledgements

The research was carried out with the grant support of the National Research Fund of Ukraine, "Information system development for automatic detection of misinformation sources and inauthentic behaviour of chat users", project registration number 187/0012 from 1/08/2024 (2023.04/0012). The research was supported by the Ministry of Internal Affairs of Ukraine "Theoretical and applied aspects of the development of the aviation sphere" under Project No. 0123U104884.

Declaration on Generative AI

The authors have not employed any Generative AI tools.

References

[1] B. Jiang, K. Zhang, Y. Lu, Q. Miao, Fault Diagnosis and Fault-Tolerant Control of Helicopters, Reference Module in Materials Science and Materials Engineering. Elsevier, 2024. doi: 10.1016/b978-0-443-14081-5.00006-4.

[2] D. Okrushko, A. Kashtalian, System of distribution and evaluation of tasks in the software development process, Computer Systems and Information Technologies 2 (2023), 86–97. doi: 10.31891/csit-2023-2-12.

[3] J. Song, Y. Wang, C. Ji, H. Zhang, Real-time optimization control of variable rotor speed based on Helicopter/ turboshaft engine on-board composite system, Energy 301 (2024) 131701. doi: 10.1016/j.energy.2024.131701.

[4] O. Balli, Exergetic, sustainability and environmental assessments of a turboshaft engine used on helicopter, Energy 276 (2023) 127593. doi: 10.1016/j.energy.2023.127593.

[5] W. Liu, G. Xu, X. Gu, J. Yao, M. Li, M. Lei, Q. Chen, Y. Fu, Experimental Analysis and Thermodynamic Modeling for Multilevel Heat Exchange System with Multifluid in Aero Engines. Energy 315 (2025) 134373. doi: 10.1016/j.energy.2025.134373.

[6] I. Tougas, M. Amani, O. Gregory, Metallic and Ceramic Thin Film Thermocouples for Gas Turbine Engines, Sensors 13:11 (2013) 15324–15347. doi: 10.3390/s131115324.

[7] M. Zoghi, N. Hosseinzadeh, S. Gharaie, A. Zare, 4E Optimization Comparison of Different Bottoming Systems for Waste Heat Recovery of Gas Turbine Cycles, Internal Combustion Engines, and Solid Oxide Fuel Cells in Power-Hydrogen Production Systems, Process Safety and Environmental Protection 187 (2024) 549–580. doi: 10.1016/j.psep.2024.04.135.

[8] M. A. Zaidan, R. F. Harrison, A. R. Mills, P. J. Fleming, Bayesian Hierarchical Models for Aerospace Gas Turbine Engine Prognostics, Expert Systems with Applications 42:1 (2015) 539–553. doi: 10.1016/j.eswa.2014.08.007.

[9] S. Ma, Y. Wu, H. Zheng, L. Gou, A Hybrid of NARX and Moving Average Structures for Exhaust Gas Temperature Prediction of Gas Turbine Engines, Aerospace 10:6 (2023) 496. doi: 10.3390/aerospace10060496.

[10] Q. Yang, B. Tang, Q. Li, X. Liu, L. Bao, Dual-Frequency Enhanced Attention Network for Aircraft Engine Remaining Useful Life Prediction. ISA Transactions 141 (2023) 167–183. doi: 10.1016/j.isatra.2023.06.020.
[11] S. Vladov, L. Scislo, V. Sokurenko, O. Muzychuk, V. Vysotska, S. Osadchy, A. Sachenko, Neural Network Signal Integration from Thermogas-Dynamic Parameter Sensors for Helicopters Turboshaft Engines at Flight Operation Conditions, Sensors 24:13 (2024) 4246. doi: 10.3390/s24134246.
[12] G. Ren, Y. Wang, Z. Shi, G. Zhang, F. Jin, J. Wang, Aero-Engine Remaining Useful Life Estimation Based on CAE-TCN Neural Networks, Applied Sciences 13:1 (2022) 17. doi: 10.3390/app13010017.
[13] B. Wang, Y. Xuan, An Integrated Model for Energy Management of Aero Engines Based on Thermodynamic Principle of Variable Mass Systems, Energy 276 (2023) 127531. doi: 10.1016/j.energy.2023.127531.
[14] Z. Long, M. Bai, M. Ren, J. Liu, D. Yu, Fault Detection and Isolation of Aeroengine Combustion Chamber Based on Unscented Kalman Filter Method Fusing Artificial Neural Network, Energy 272 (2023) 127068. doi: 10.1016/j.energy.2023.127068.
[15] K. Wang, Y. Guo, W. Zhao, Q. Zhou, P. Guo, Gas Path Fault Detection and Isolation for Aero-Engine Based on LSTM-DAE Approach under Multiple-Model Architecture, Measurement 202 (2022) 111875. doi: 10.1016/j.measurement.2022.111875.
[16] J. Liu, F. Lei, C. Pan, D. Hu, H. Zuo, Prediction of Remaining Useful Life of Multi-Stage Aero-Engine Based on Clustering and LSTM Fusion, Reliability Engineering & System Safety 214 (2021) 107807. doi: 10.1016/j.ress.2021.107807.
[17] S. Vladov, L. Scislo, V. Sokurenko, O. Muzychuk, V. Vysotska, A. Sachenko, A. Yurko, Helicopter Turboshaft Engines' Gas Generator Rotor R.P.M. Neuro-Fuzzy On-Board Controller Development, Energies, 17:16 (2024), 4033. doi: 10.3390/en17164033.
[18] R. M. Catana, G. Dediu, Analytical Calculation Model of the TV3-117 Turboshaft Working Regimes Based on Experimental Data, Applied Sciences 13:19 (2023) 10720. doi: 10.3390/app131910720.
[19] C. M. Stefanovic, A. G. Armada, X. Costa-Perez, Second Order Statistics of -Fisher-Snedecor Distribution and Their Application to Burst Error Rate Analysis of Multi-Hop Communications, IEEE Open Journal of the Communications Society 3 (2022), 2407–2424. doi: 10.1109/ojcoms.2022.3224835.
[20] H.-Y. Kim, Statistical notes for clinical researchers: Chi-squared test and Fisher's exact test, Restorative Dentistry & Endodontics 42:2 (2017) 152. doi: 10.5395/rde.2017.42.2.152.
[21] B. Rusyn, O. Lutsyk, R. Kosarevych, O. Kapshii, O. Karpin, T. Maksymyuk, J. Gazda, Rethinking Deep CNN Training: A Novel Approach for Quality-Aware Dataset Optimization, IEEE Access 12 (2024) 137427–137438. doi: 10.1109/access.2024.3414651.
[22] L. Wang, H. Zhang, C. Wang, Deep Neural Network-Based Modeling of Multimodal Human–Computer Interaction in Aircraft Cockpits, Future Internet 17:3 (2025) 127. doi: 10.3390/fi17030127.
[23] S. Vladov, A. Sachenko, V. Sokurenko, O. Muzychuk, V. Vysotska, Helicopters Turboshaft Engines Neural Network Modeling under Sensor Failure, Journal of Sensor and Actuator Networks 13:5 (2024) 66. doi: 10.3390/jsan13050066.
[24] S. Hassantabar, Z. Wang, N. K. Jha, SCANN: Synthesis of Compact and Accurate Neural Networks, IEEE Transactions on Computer-Aided Design of Integrated Circuits and Systems 41:9 (2022), 3012–3025. doi: 10.1109/tcad.2021.3116470.
[25] I. Perova, Y. Bodyanskiy, Fast medical diagnostics using autoassociative neuro-fuzzy memory, International Journal of Computing 16:1 (2017) 34–40. doi: 10.47839/ijc.16.1.869.